Fast Evaluation of Electromagnetic Interference Between Antenna and PCB Traces for Compact Mobile Devices

S. Grivet-Talocia*, M. Bandinu†, F. G. Canavero*, I. Kelander‡, and P. Kotiranta‡
*Politecnico di Torino, Dip. Elettronica, Torino, Italy. E-mail: stefano.grivet@polito.it
†IdemWorks s.r.l., Torino, Italy. E-mail: michelangelo.bandinu@idemworks.com
‡NOKIA Corporation, Helsinki, Finland. E-mail: ilkka.kelander@nokia.com

***Abstract*—This paper proposes a technique for the fast evaluation of antenna-induced noise at the terminations of PCB traces on compact mobile phones platforms. The main approach is based on the classical theory of transmission lines with external field excitation. We show that a single full-wave electromagnetic simulation is needed to compute the coupling coefficients for an arbitrary location of the trace on the phone PCB. Therefore, the approach is ideally suited for the automated incorporation of EMI constraints within routing and placement algorithms and for parametric and what-if analyses.**

I. Introduction

The design flow of modern mobile phones has become a quite challenging task, due to serious Electromagnetic Compatibility (EMC) issues. Even low-cost devices have nowadays multiple antennas transmitting a significant amount of power on different frequency bands, up to multi-GHz. The intentional electromagnetic field produced by these antennas results in a noisy environment for the very close and potentially very sensitive devices located on the phone Printed Circuit Board (PCB). Therefore, a careful assessment of the noise induced by the phone antennas at the input/output ports of the PCB digital drivers and receivers is mandatory to make sure that no false switching occurs due to a noise margin violation.

A brute-force approach for the estimation of the antenna-induced noise at the terminations of a PCB trace would require a global full-wave electromagnetic simulation of the entire structure, including all geometry/material details that have some influence on the results. Unfortunately, this approach may result quite time-consuming despite the compact dimensions of the phone. This is mainly due to the very fine resolution that would be needed for meshing the cross-section of the PCB trace in order to obtain reliable results. Moreover, different locations of the PCB trace would require entirely new field simulations, leading to prohibitive problem setup and simulation times for an automated design flow, e.g., for parametric/what-if studies and automated routing under minimal EMI constraints.

We suggest a different approach based on the well-established theory of field-excited transmission lines. This approach requires only one global full-wave field simulation of the bare phone structure including power/ground planes but without the victim trace. Therefore, no fine geometrical details are present, allowing for coarse mesh settings and fast simulation times. The results of this simulation are then post-processed for computing the coupling coefficients at the termination of the trace, for any arbitrary location on the phone PCB.

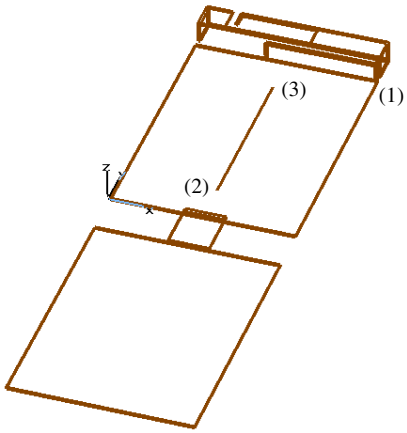

Fig. 1. Simplified geometry of a mobile phone with electrical ports definition.

We conduct our investigations on a simplifed but realistic clam-shell phone structure. All geometrical details are provided in Section II. The modeling approach is detailed in Section III. Finally, results and validations are provided in Section IV.

II. Problem description

This section presents the structure that we will use troughout this paper for illustration and validation of the proposed approach. Figure 1 shows the skeleton of a clam-shell phone, and Table I provides the relevant dimensions. The geometry specification includes the ground planes of the two main phone parts, which are connected by a hinge, and the GSM antenna. The feed of the antenna is located at the corner of the top ground plane. The PCB is modeled with a single signal layer on a lossless dielectric substrate with relative permettivity $\varepsilon_r = 4.7$ and height $h = 0.06$ mm. Copper material (conductivity $\sigma = 5.8 \times 10^7$ S/m) is used for all conducting bodies.

Three electrical ports can be defined for this structure. Their

978-1-4244-1699-8/08/$25.00 ©2008 IEEE

TABLE I
GEOMETRY AND MATERIAL SPECIFICATIONS.

Component	Width	Length	Thickness	Material
Ground plane 1	45 mm	60 mm	0.5 mm	Copper
Ground plane 2	45 mm	60 mm	0.5 mm	Copper
Hinge	10 mm	12 mm	0.5 mm	Copper
Trace	0.1 mm	40 mm	0.03 mm	Copper

numbering will be consistent throughout this paper. Port #1 is the antenna feed, whereas ports #2 and #3 denote the terminations of a PCB trace, which is routed on the first PCB, with arbitrary corner points. Main objective of this paper is to provide a fast evaluation of the scattering matrix elements S_{21} and S_{31} as functions of frequency and routing path of the PCB trace.

We remark that the generalization of this approach to multiple antennas transmitting simultaneously and to multiple concurrent traces is trivial using standard superposition arguments. Therefore, our presentation will focus on a single trace and single transmitting antenna, corresponding to a 3-port system.

III. METHODOLOGY

The proposed approach is based on the representation of the PCB trace as a field-excited transmission-line, whose electrical variables satisfy the nonhomogeneous Telegraphers' equations

$$\frac{d}{d\nu}V(\nu,\omega) + Z(\omega)I(\nu,\omega) = V_F(\nu,\omega), \tag{1}$$

$$\frac{d}{d\nu}I(\nu,\omega) + Y(\omega)V(\nu,\omega) = I_F(\nu,\omega), \tag{2}$$

where ν is the longitudinal coordinate along the routing path of the trace, $V(\nu,\omega)$ and $I(\nu,\omega)$ are frequency-domain voltage and current along the line, $Z(\omega)$ and $Y(\omega)$ are the per-unit-length transverse impedance and admittance. These parameters are easily computed using a 2D field solver. We adopt here a Method-of-Moments (MoM) techinque based on [3] and [4]. The forcing terms $V_F(\nu,\omega)$, $I_F(\nu,\omega)$ represent distributed sources along the line and are due to the interfering electromagnetic field surrounding the line.

Several formulations of the field-to-line coupling for the evaluation of $V_F(\nu,\omega)$, $I_F(\nu,\omega)$ are available in the open literature [1]. All such formulations are obtained via some derivation of the Telegraphers' equations (1)-(2) from Maxwell's equations. Following [1], we adopt the following definition of the distributed sources, originally due to Agrawal [2]

$$V_F(\nu,\omega) = -\frac{d}{d\nu}\int_a^b \underline{\mathcal{E}}_t^i \cdot \underline{dl} + \mathcal{E}_\nu^i\big|_b - \mathcal{E}_\nu^i\big|_a\,, \tag{3}$$

$$I_F(\nu,\omega) = -Y(\omega)\int_a^b \underline{\mathcal{E}}_t^i \cdot \underline{dl}\,. \tag{4}$$

where a, b are two points on the PCB reference (ground) plane and on the trace, respectively. The *incident* electric field $\mathcal{E}^i$ is defined as the externally-excited field (in present case by the radiating phone antenna) in presence of the return (ground) conductor, with the trace removed. Subscripts ν and t denote the longitudinal and transverse components of the field, always with respect to the line routing path. Formulation (3)-(4) is preferred here with respect to other solutions, since no information on the magnetic field is required.

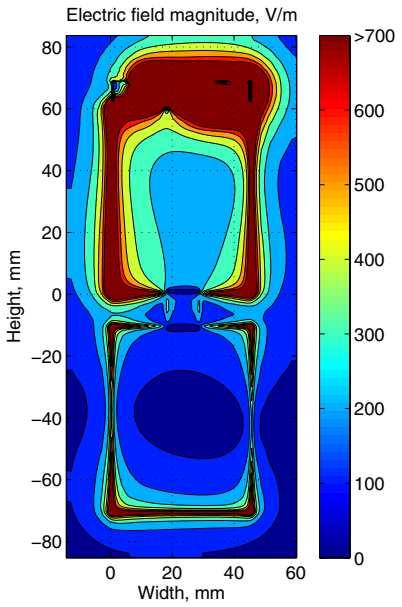

Fig. 2. Incident field (magnitude) @1800 MHz, computed with the PCB trace removed.

A. Incident Fields Computation

The three components of the incident electric field $\mathcal{E}^i$ are computed in a pre-processing phase using a full-wave solver. In this work, we have used a time-domain solver [5] combined by Fast Fourier Transform postprocessing in order to derive the frequency samples of the incident field. However, any solver can be used in principle for this task. The full-wave solution is setup by removing the trace conductor, and by exciting the antenna with a unit power source with some prescribed internal impedance R_0.

Due to the absence of the PCB trace, the mesh settings need not to be very aggressive. The only constraint is dictated by an accurate evaluation of (3) and (4). A closer look at these expressions leads to the following considerations

- The transverse component of the incident field $\mathcal{E}_t^i$ always appears as a line integration in the dielectric space between the reference and the signal (trace) conductor. A natural choice is to select the shortest integration path, which is orthogonal to the ground plane in this case. Since the trace is very close to the ground, it is sufficient to have two mesh points on the ground (a) and trace surface (b), for a correct enforcement of the boundary conditions. No other mesh points are needed in the space between ground and trace. The variation of the incident field from a to b can be safely assumed to be negligible, therefore the line integral is readily obtained as $h\ \mathcal{E}_t^i\big|_b$, where h is the height of the trace above the ground plane.

- The longitudinal component of the incident field on the ground plane $\mathcal{E}^i_\nu\big|_a$ is vanishing due to the boundary conditions. Therefore, only the longitudinal component on the trace $\mathcal{E}^i_\nu\big|_b$ need to be stored.

In summary, only the samples of the electric field at the location of the trace are needed. If a 2D grid of samples covering with sufficient resolution the entire plane parallel to the ground at height h are stored, the distributed sources (3) and (4) can be computed as a post-processing step for any routing path.

Figure 2 reports a map of the incident electric field excited by the antenna with the PCB trace removed, computed on a plane at height $h = 0.06$ mm from the ground plane. This is the input data for the evaluation of the coupling coefficients for any arbitrary location of the trace, as discussed above. The field data is obtained by a single full-wave simulation using [5]. Only a CPU time of 2 hours was required by this simulation on a standard notebook. Note also that the evaluation of the distributed sources according to the above formulation requires negligible CPU time with respect to the field solution time.

B. Coupling Coefficients

Once the distributed sources are available, the coupling coefficients S_{21} and S_{31} are readily computed using standard transmission-line theory. First, equations (1)-(2) are solved as illustrated in [1] in order to compute their non-homogeneous chain matrix representation

$$\begin{bmatrix} V_1(\omega) \\ I_1(\omega) \end{bmatrix} = \begin{bmatrix} \Phi_{11}(\omega) & \Phi_{11}(\omega) \\ \Phi_{11}(\omega) & \Phi_{11}(\omega) \end{bmatrix} \begin{bmatrix} V_2(\omega) \\ I_2(\omega) \end{bmatrix} + \begin{bmatrix} V_{FT}(\omega) \\ I_{FT}(\omega) \end{bmatrix}, \quad (5)$$

where subscripts $_{1,2}$ denote voltages and currents at near and far end of the line, respectively. Detailed expressions for the chain matrix parameters $\Phi_{ij}(\omega)$ and the lumped sources $V_{FT}(\omega)$, $I_{FT}(\omega)$ can be found in [1]. Terminating the line with identical impedances

$$V_1(\omega) = -R_0 I_1(\omega), \quad V_2(\omega) = R_0 I_2(\omega) \quad (6)$$

and solving the resulting linear system at each frequency value leads to the desired scattering matrix elements $S_{21}(\omega)$ and $S_{31}(\omega)$.

We remark that $S_{11}(\omega)$ is already available from the reference simulation that we used to determine the incident field, since only port #1 is excited. In addition, the four elements $S_{ij}(\omega)$ with $i = 2, 3$ and $j = 2, 3$ correspond to the scattering matrix of the transmission line with no field excitation and can be obtained from the chain matrix $\mathbf{\Phi}(\omega)$ above using standard conversion formulas. Reciprocity arguments allow to fill the 3×3 scattering matrix in order to recover the complete set of responses of our 3-port system.

C. Discussion

Of course, there are several approximations involved in the proposed approach. Most important assumptions are

- There is a negligible interaction between the trace and the antenna, so that the one-way coupling approximation can be performed. For the problem under investigation the coupling coefficients are small enough for this approximation to be feasible well within engineering accuracy.
- The antenna-mode current along the line is intrinsically neglected in this formulation, since Telegraphers' equations are used.
- The presence of bends along the line routing path is not considered, since the trace is regarded as a single uniform transmission-line segment. However, the generalization to this case is rather simple, since a cascaded model of several straight segments separated by suitable lumped equivalents of the bends may be used. In any case, the numerical results of Section IV show that for this example and for the considered range of frequencies, bends do not have a significant influence on the results.
- Propagation along the line follows the quasi-TEM mode and no higher modes are considered. This assumption is certainly satisfied due to the very small cross-section of the trace.

A careful validation campaign has been conducted for several configurations, to make sure that these approximations are not neglecting important physical phenomena. The results of these validations are reported in Section IV.

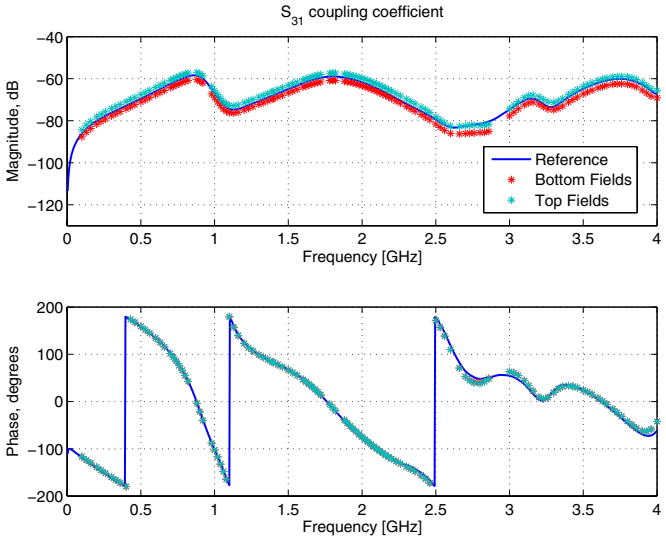

Fig. 3. Coupling coefficient S_{31} for the straight trace geometry of Fig. 1. The results obtained using incident fields at height $h = 0.06$ mm (bottom) and $h = 0.09$ mm (top) above the ground plane are compared to the reference results obtained with a global full-wave simulation, including the PCB trace.

IV. Numerical Results

We present here a set of numerical validations to demonstrate the feasibility of our approach. Two different trace routing configurations are considered. The first case corresponds to the geometry depicted in Fig. 1, with the trace located at the center of the ground plane adjacent to the antenna. Figure 3 reports the coupling coefficient S_{31} (similar results were obtained for S_{21}, not shown) as functions of frequency. The blue solid curves represent the benchmark solutions, obtained

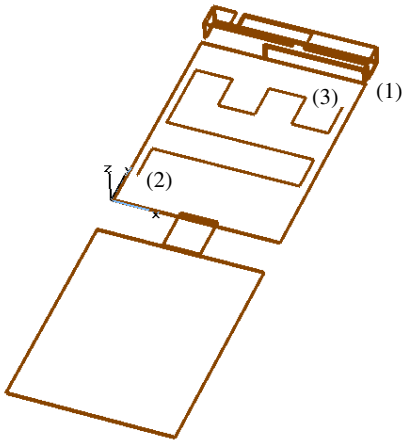

Fig. 4. Complex trace routing path used for validation.

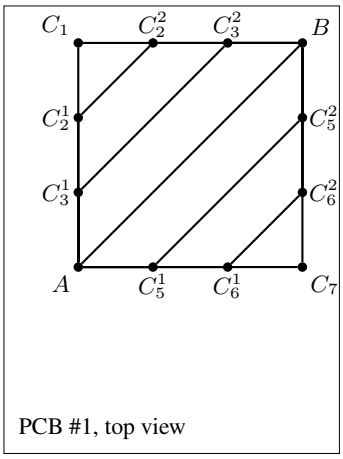

Fig. 6. A parameterized trace routing path between end points A and B. A variable number j of corners C_i^j is allowed for path i, with only 90-degree and 45-degree turns. Seven paths are considered, namely: AC_1B, $AC_2^1C_2^2B$, $AC_3^1C_3^2B$, AB, $AC_5^1C_5^2B$, $AC_6^1C_6^2B$, AC_7B.

by a full-wave solution of the entire structure including the PCB trace. The star marks report the results obtained with the proposed approach. Two sets of results are reported. First set is obtained using the samples of the incident field at height $h = 0.06$ mm above the ground plane, corresponding to the bottom surface of the trace. The second set is instead obtained setting $h = 0.09$ mm, at the top surface of the trace. These two sets may be used to assess the sensitivity of the numerical technique to the mesh settings used for the incident field computation. The general agreement is excellent. We remark that the CPU time required for the evaluation of the reference curves (using [5]) was more than 10 hours, whereas the computation of the coupling coefficients required only few seconds for the full frequency sweep.

A second example with a more complex geometry is now considered in order to investigate the effects of a nonuniform routing path with bends. The example is deliberately non-realistic, with the aim of stressing the main assumptions. The geometry is reported in Fig. 4, whereas the corresponding validation plots are depicted in Fig. 5. Despite the presence of several 90-degree bends and several parallel segments of the trace, the proposed approach leads to very reasonable results, since the obtained level of accuracy is comparable with the results for the straight case.

The above results validate the proposed methodology. Next example provides a possible application scenario. The routing path of the PCB trace is varied by parameterizing some of the routing points. In particular, the path between the end points is split into straigth segments with only 45-degree or 90-degree turns, with a varying number of corner points. A graphical illustration of the investigated parameter space for this test is provided in Fig. 6.

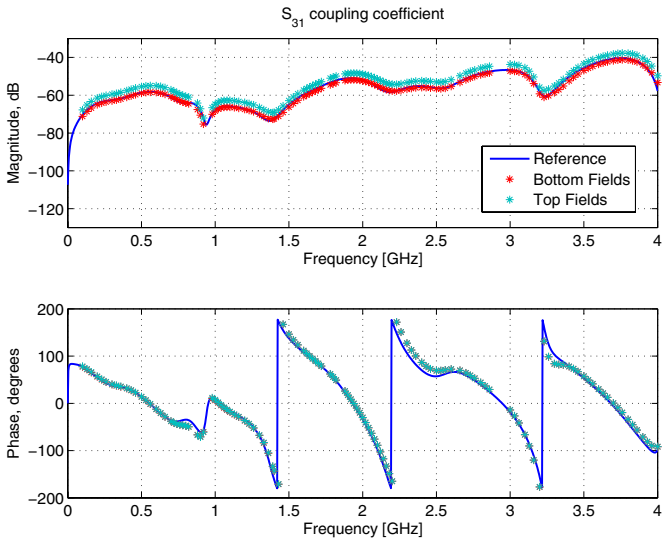

Fig. 5. As in Fig. 3, but for the geometry depicted in Fig. 4.

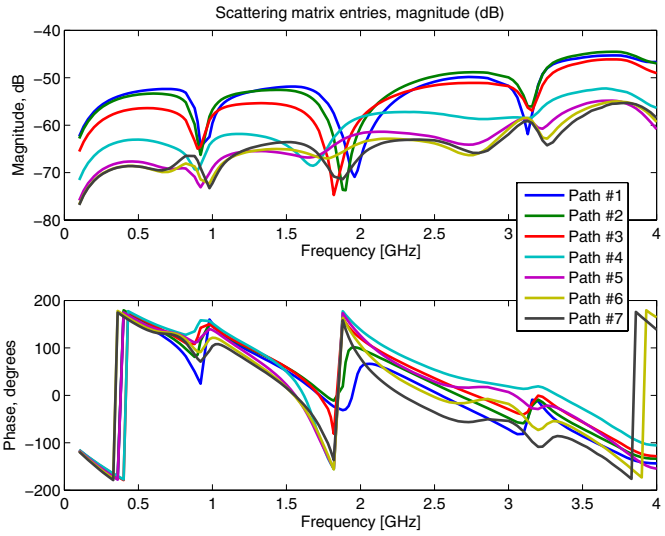

Fig. 7. Parameterized coupling coefficients for the various routing paths depicted in Fig. 6.

Iterative application of the coupling coefficients evaluation scheme leads to the results depicted in Fig. 7, where these coefficients are plotted as functions of both frequency and routing path configuration. No additional full-wave simulations are required for this task, resulting in a full parametric assessment of the coupling, which can be performed in few seconds. It is clear that the high numerical efficiency of this methodology allows a direct insertion of the coupling coefficients as cost functions in the routing and placement optimization run for several traces, thus allowing for a direct inclusion of self-EMI constraints in the design of the phone physical layout. This will be the next step of this investigation.

REFERENCES

[1] C. Paul, *Analysis of Multiconductor Transmission Lines*, Wiley, 2nd Ed., 2007.

[2] A. K. Agrawal, H. J. Price, and S. H. Gurbaxani, "Transient response of multiconductor transmission-lines excited by a nonuniform electromagnetic field," *IEEE Trans. Electromagn. Compat.*, vol. 22, pp. 119-129, May 1980.

[3] C. Wei, R. F. Harrington, J. R. Mautz, T. Sarkar, "Multiconductor Transmission Lines in Multilayered Delectric Media", *IEEE Trans. Microwave Theory and Techniques*, Vol. 32, N. 4, Apr. 1984, pp. 439–450.

[4] K. M. Coperich, J. Morsey, V. I. Okhmatovski, A. C. Cangellaris, A. E. Ruehli, "Systematic development of transmission-line models for interconnects with frequency-dependent losses" *IEEE Trans. Microwave Theory and Techniques*, Vol. 49, N. 10, Oct. 2001, pp. 1677–1685.

[5] *CST Microwave Studio* (www.cst.de)